Mass-15 nuclei and predicting narrow states beyond the proton drip line

P. R. Fraser,[1,*] K. Amos,[2,4,†] L. Canton,[3,‡] S. Karataglidis,[4,§] D. van der Knijff,[2,‖] and J. P. Svenne[5,¶]

[1]*School of Science, and Learning and Teaching Group, The University of New South Wales, Canberra, ACT 2600, Australia*

[2]*School of Physics, University of Melbourne, Victoria 3010, Australia*

[3]*Istituto Nazionale di Fisica Nucleare, Sezione di Padova, via Marzolo 8, Padova I-35131, Italy*

[4]*Department of Physics, University of Johannesburg, P.O. Box 524, Auckland Park 2006, South Africa*

[5]*Department of Physics and Astronomy, University of Manitoba, and Winnipeg Institute for Theoretical Physics, Winnipeg, Manitoba R3T 2N2, Canada*

(Received 14 October 2017; revised manuscript received 10 January 2019; published 12 August 2019)

In a previous Letter [Phys. Rev. Lett. **96**, 072502 (2006)], the multichannel algebraic scattering (MCAS) technique was used to calculate spectral properties for proton-unstable ^{15}F and its mirror, ^{15}C. This achieved a close match to the then-new data for $p + {}^{14}$O elastic scattering and predicted several unusually narrow resonances at higher energies. Subsequently, such narrow resonance states were discovered. New cross section data has been published characterizing the shape of the $J^\pi = \frac{1}{2}^-$ resonance. Herein we update that first MCAS analysis and its predictions. We also study the spectra of the set of mass-15 isobars ^{15}C, ^{15}N, ^{15}O, and ^{15}F, using the MCAS method seeking a consistent Hamiltonian for clusterization with a neutron and a proton, separately, coupled to core nuclei ^{14}C and ^{14}O.

DOI: 10.1103/PhysRevC.100.024609

I. INTRODUCTION

The low-energy spectra of exotic, light-mass nuclei beyond the drip lines have been the foci of intense research efforts since the advent of radioactive ion beams. The nucleus ^{15}F has been of special interest both because it spontaneously emits a proton and for the role played by that reaction in the $2p$ decay of ^{16}Ne.

Herein we report on results of calculations of the low energy spectra of the mass-15 isobars ^{15}C, ^{15}N, ^{15}O, and ^{15}F. These nuclei are disparate in that ^{15}O and ^{15}N have deep binding and many fully bound states in their low energy spectra, while ^{15}C is weakly bound with only two subthreshold (to neutron emission) states and ^{15}F is unbound (to proton emission). To describe the low energy spectra of these systems with a single, simple Hamiltonian is the difficult aim we set. However, a primary focus under this aim is to predict the existence and location of more states in the exotic nucleus, ^{15}F, than are currently known. Regarding this nucleus, in 2002 a $p + {}^{14}$O Wood-Saxon potential was parametrized [1] to find the energies and widths of the only two ^{15}F states then known: the ground $J^\pi = \frac{1}{2}^+$ and first excited $\frac{5}{2}^+$ resonances. That potential, used in a three-body model for ^{16}Ne, proved useful in recent analyses of two-proton decay data [2,3]. In 2004, the first ^{14}O$(p, p)^{14}$O cross section data taken at several angles and at energies spanning the two known resonance states were published [4]. In that paper, data fits found using Woods-Saxon potentials were shown. The next year, these data were analyzed with a microscopic cluster model, which obtained a good match [5], and further data were soon taken and published [6]. In the same year, properties of these two ^{15}F states were studied with a simplistic shell model [7]. This model was restricted to the lowest three configurations of one-particle/two-hole and three-particle/four-hole states.

In 2006, the multichannel algebraic scattering method (MCAS) was used to analyze the data of Refs. [4,6], defining potentials between ^{14}O and protons from a collective model with rotor character, while accounting for the Pauli principle between the proton and the underlying ^{14}O shell structure [8]. As well as obtaining a close fit with the cross section data, the calculation predicted narrow resonances at higher energies. These were a $\frac{1}{2}^-$ state with energy (width) of 5.49 (0.005) MeV, a $\frac{5}{2}^-$ of 6.88 (0.01) MeV, a $\frac{3}{2}^-$ of 7.25 (0.04) MeV, as well as $\frac{1}{2}^+$, $\frac{5}{2}^+$, and $\frac{3}{2}^+$ states of 7.21 (1.2), 7.75 (0.4), and 7.99 (3.6) MeV, respectively.

The widths of such narrow states caused some controversy [9,10] (with Ref. [9] using a potential model to construct broad single-particle resonances whose widths were manually scaled down by over an order of magnitude to fit data for narrow resonances). Subsequently, however, the existence of the states predicted by the MCAS calculation was verified experimentally [11–13]. (Note that in Table I of Ref. [13], the labels for results reproduced from Refs. [8] and [9] were accidentally switched.) For completeness we note that ^{15}C and thus ^{15}F widths in the aforementioned simple shell model calculation were revised [14] in the light of the new data.

*paul.fraser@unsw.edu.au
†amos@unimelb.edu.au
‡luciano.canton@pd.infn.it
§stevenka@uj.ac.za
‖dvanderknijff@gmail.com
¶svenne@physics.umanitoba.ca

Narrow states have now been observed in other proton rich nuclei, e.g., ^{19}Na [15], ^{16}Ne [13], ^{15}Ne [16], and ^{23}Al [17], with narrow resonances of the latter found with an MCAS study [18]. They have been predicted for ^{21}Al [19] and ^{25}P [20]. Such narrow resonances indicate an eigenstate with little overlap with the ground state. In the case at hand, this is the difference between a one-proton emitting clusterization ($p + ^{14}$O) and a two-proton emitting clusterization ($2p + ^{13}$N). Pauli hindrance accounts for this effect [21].

Recent developments include the publication of more complete data with smaller uncertainties over a larger energy range [22–24]. Where Ref. [13] provided evidence of the narrow $\frac{1}{2}^-$ resonance predicted by MCAS, Ref. [24] provides details of its shape, finding it to be a dip in cross section, in agreement with the prediction of Ref. [8]. Further, in Ref. [24] and in a recently published thesis [25], the coupled-channels Gamow shell model (GSM-CC) [26] was used to calculate the ^{14}O$(p, p)^{14}$O cross section, reproducing the $\frac{1}{2}^+$, $\frac{5}{2}^+$, and $\frac{1}{2}^-$ resonances well. At higher energies, that calculation slightly underestimates experiment.

As MCAS theory has undergone a decade of refinement since Ref. [8], we now take the opportunity presented by these new data to revisit our calculation in the energy range where cross sections have been measured and beyond, where the method predicts further resonances. Section II summarizes the method and details improvements since the work of Ref. [8]. Section III presents calculated results for the spectra of the mirror systems ^{15}C and ^{15}F. Section IV shows the new $p + ^{14}$O cross section results compared to recent data. In Sec. V, we investigate how many details of the spectra of another mass-15 mirror pair, ^{15}O and ^{15}N, may be described by essentially the same nuclear potential, i.e., that for $n + ^{14}$O and $p + ^{14}$C. The impact of the choice of target-state channels and the influence of the Pauli principle upon the coupled-channel calculations is then considered in Sec. VI. Finally, conclusions are drawn in Sec. VII.

II. DETAILS OF THE METHOD

The method finds solutions of coupled-channel Lippmann-Schwinger equations in momentum space using finite-rank expansions of an input matrix of nucleon-nucleus interactions. A set of Sturmian functions is used as an expansion basis and this allows location of all compound-system resonance centroids and widths, regardless of how narrow. Subthreshold bound states can be determined by solving the coupled Sturmian eigenvalue equation at negative energies. Further, use of orthogonalizing pseudopotentials (OPP) in generating the Sturmians ensures that the Pauli principle is not violated [27,28], even with a collective-model formulation of nucleon-nucleus interactions. Otherwise, some compound nucleus wave functions may possess spurious components [29].

Results we have obtained vary slightly from those previously published [8] since five target (or core) nuclear states now have been used in the coupled-channel evaluations (rather than the three in Ref. [8]), and concomitantly the interaction potential parameters have been adjusted slightly, and exact masses of the nucleons and nuclei used rather than the mass numbers. Further, the Coulomb interactions in the $p + ^{14}$O

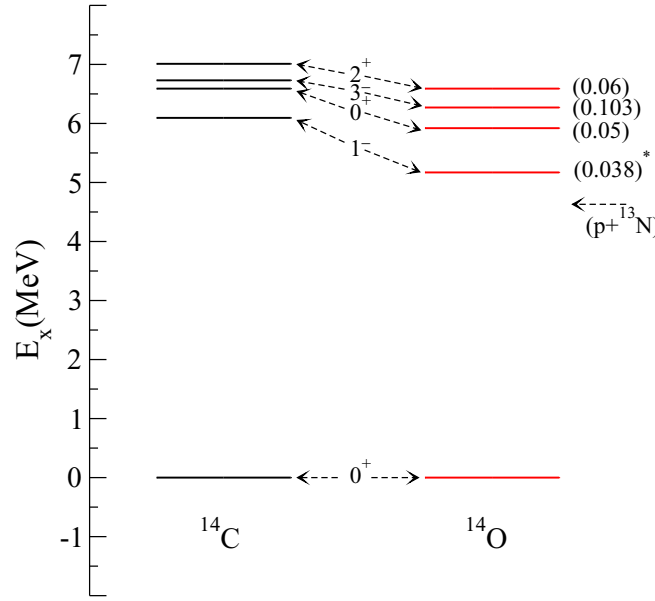

FIG. 1. The low excitation spectra of the mass-14 mirror nuclei ^{14}C and ^{14}O used in MCAS calculations. The spin-parities of the states are listed in the middle of the diagram.

cluster has been derived from a three-parameter Fermi (3pF) form for the charge distribution in ^{14}O, adding to the nuclear interaction which has the form

$$V_{cc'}(r) = \left[\{V_0 + V_{ll}\ell\cdot\ell\}f(r,R,a) + V_{\ell\cdot s}\frac{df(r,R,a)}{dr}\ell\cdot s\right]_{cc'}. \quad (1)$$

Here $f(r, R, a)$ is a deformed Woods-Saxon function, and both quadrupole and octupole deformations are taken to second order in specifying the coupled-channel (c, c') potentials.

For full details, see [27,30].

A. States used for the core nuclei, ^{14}C and ^{14}O

In Fig. 1, the known low-energy spectra of the mirror nuclei ^{14}C and ^{14}O are shown. These states have all been used in the current coupled-channel calculations. (See Sec. VI A for the impact of adding each state.) While the sequence of each of the states shown (the spin-parities) are as required by the mirror condition and the excitation energies are comparable, there are features that vary from a strict mirror arrangement. Notably, the actual excitation energies of the states in ^{14}O differ from those of their matching partners in ^{14}C, as do the energy gaps, but also the relative nucleon breakup energies are quite different: 8.176 MeV for neutron emission from ^{14}C but only 4.628 MeV for a proton emission from ^{14}O. Consequently the four excited states in ^{14}O are resonances while those in ^{14}C are not. The widths of the four ^{14}O resonances are shown in brackets in Fig. 1, and the units are MeV. The asterisk with the width of the first excited (1^-) resonance indicates that its emission form is not identified in the tabulation used [31]. The other three all decay by proton emission. For details of how MCAS treats core nuclei states which are themselves resonances, see Refs. [32–34]. This

represents another upgrade with respect to the calculation originally published [8].

As the two cores used in these coupled-channel, nucleon-nucleus cluster calculations do not show perfect mirror symmetry even at low excitation, one may expect the possibility of some asymmetry between the two Hamiltonians required to best define the relative mass-15 spectra, in addition to simply a Coulomb interaction added to the cluster model Hamiltonian that best describes the ^{15}C spectrum. Some added asymmetry may be due to a charge dependence of the strong force. Such considerations lie behind the development of the isospin nonconserving shell model [35].

That charge dependence results in differences between the two mirror nuclei considered is suggested by the disparity in the log-ft quantity obtained from studies of β decay [36]. ^{14}C has an unusually large log-ft value of 9.04, while its mirror, ^{14}O, has a value of 3.4892. Thus, while the difference in ground state energies is only 80 keV, the wave functions may not be exact mirrors. The spectra are similar, but the first excited state energies differ by 920 keV. As a result, while this indicates that there may be a difference in energy due to Coulomb effects, one cannot estimate it with any certainty due to the anomalous log-ft value for ^{14}C. No shell model wave function has been able to reproduce that large value [37].

In this investigation, these differences are taken into account by (small) variations in the OPP parameters. (See Sec. II C.)

B. The charge distribution and electromagnetic properties

For any nuclear charge distribution, electric multipole operators are defined in the space-fixed frame by

$$T_{\lambda\mu} = \int \rho_0 \rho_{ch}(\mathbf{r})\, r^{\lambda} Y^{\star}_{\lambda\mu}(\theta,\phi)\, d\mathbf{r}. \tag{2}$$

Here $\mu\hbar$ is the angular momentum projection on the space-fixed z axis, and ρ_0 is the central charge density value, $\rho_0 = Ze/[4\pi \int \rho_{ch}(r) r^2 dr]$.

We suppose that the nucleus is like an incompressible liquid drop whose surface, $R(\theta,\phi)$, can be deformed. Expanding that surface to first order gives

$$R(\theta\phi) = R_0 \left[1 + \sum_{\lambda\mu} \alpha^{\star}_{\lambda\mu} Y_{\lambda\mu}(\theta\phi) \right]. \tag{3}$$

Then any function with that surface can also be expanded as

$$F(\mathbf{r}) = F(r) - R_0 \frac{dF}{dr} \sum_{\lambda\mu} \alpha^{\star}_{\lambda\mu} Y_{\lambda\mu}(\theta\phi), \tag{4}$$

and, in particular, the nuclear charge distribution as

$$\rho_0 \rho_{ch}(\mathbf{r}) = \rho_0\, \rho_{ch}(r) - \rho_0 R_0 \left(\frac{d\rho_{ch}(r)}{dr} \right) \sum_{lm} \alpha^{\star}_{lm} Y_{lm}(\Omega). \tag{5}$$

Substituting Eq. (5) in Eq. (2) gives

$$\begin{aligned} T_{\lambda\mu} &= \int \rho_0 \rho_{ch}(\mathbf{r})\, r^{\lambda} Y^{\star}_{\lambda\mu}(\theta\phi)\, d\mathbf{r} \\ &= -\rho_0\, R_0 \int_0^{\infty} r^{\lambda+2} \left(\frac{d\rho_{ch}(r)}{dr} \right) dr\, \alpha^{\star}_{\lambda\mu}\,. \end{aligned} \tag{6}$$

Quantization with the collective vibration model is then made using the transformation

$$\alpha^{*}_{\lambda\mu} \rightarrow \beta_{\lambda} \frac{1}{\sqrt{(2\lambda+1)}} \{ b^{\dagger}_{\lambda\mu} + (-)^{\mu} b_{\lambda-\mu} \}; \tag{7}$$

$b^{\dagger}_{\lambda\mu}$ and $b_{\lambda-\mu}$ are phonon creation and annihilation operators and β_{λ} are coupling strengths.

First-order expansions suffice for transitions between pure vibration model states: the ground as the vacuum ($|0,0\rangle$), and the 2^+_1 and 3^-_1 ones being a single quadrupole and single octupole phonon excitation upon that vacuum, $b^{\dagger}_{2\mu}|0,0\rangle$ and $b^{\dagger}_{3\nu}|0,0\rangle$ respectively. Electromagnetic transitions between the ground state and the single-phonon excited states have matrix elements of the form

$$\begin{aligned} \langle J_f M_f | \alpha^{\star}_{J_f M_f} | 0,0 \rangle &= \langle 0,0 | b_{J_f M_f}\ \beta_{\lambda} \frac{1}{\sqrt{2J_f+1}} b^{\dagger}_{J_f M_f}\ |0,0\rangle \\ &= \frac{1}{\sqrt{2J_f+1}} \beta_{J_f}, \end{aligned} \tag{8}$$

with which the electromagnetic transition probabilities are

$$B(E\lambda) = \sum_{M_f} |\langle J_f M_f | T_{\lambda\mu} | 00 \rangle|^2 = |\langle J_f || T_{\lambda} || 0 \rangle|^2, \tag{9}$$

where $\lambda = J_f$. For the finite distribution of charge, these transition probabilities are given by

$$B(E\lambda)\uparrow = \frac{1}{(2J_f+1)} \beta^2_{J_f}\, \rho_0^2\, R_0^2 \left[\int_0^{\infty} r^{\lambda+2} \left(\frac{d\rho_{ch}(r)}{dr} \right) \right]^2. \tag{10}$$

We use this pure vibration model to describe the states of ^{14}O in coupled-channel evaluations of the spectra of ^{15}F treated as the $p + {}^{14}$O cluster, and of low-energy scattering of ^{14}O ions from hydrogen. Quadrupole and octupole coupling constants are involved in defining the matrix of interaction potentials to be used, and for these we seek guidance from electromagnetic properties of the "target." The relevant $B(E2)\uparrow$ and $B(E3)\uparrow$ values in ^{14}O are as yet unknown, while those values for the transitions in ^{14}C are uncertain, though, from that $B(E2)$ value, Raman [38] gives an adopted value of $\beta_2 = 0.36$ [the sign being ambiguous since $B(E2)$ depends on β_2^2]. However, we assume that both the $E2$ and $E3$ transitions in ^{14}O would be similar to those in ^{16}O, namely $\approx 40\ e^2\text{fm}^4$ [38] and $\approx (1300\text{–}1500)\ e^2\text{fm}^6$ [39] respectively.

We have used a 3pF model for the charge distribution in ^{14}O, viz.,

$$\rho_{ch}(r) = \frac{1 + w_c \left(\frac{r^2}{R_c^2} \right)}{1 + \exp\left(\frac{r - R_c}{a_c} \right)}. \tag{11}$$

As reported in Ref. [40], electron scattering form factors, when used to specify a 3pF charge distribution for ^{16}O, set the parameter values as $R_c, a_c, w_c = 2.608$ fm, 0.52 fm, -0.051. We presuppose that the charge distribution in ^{14}O would be slightly more diffuse and have used the set $R_c, a_c, w_c =$ 2.59 fm, 0.6 fm, -0.051. With that distribution, the $B(E2)\uparrow$ with $\beta_2 = 0.36$ is 45.6 $e^2\text{fm}^4$; cf. 40.6 $e^2\text{fm}^4$ adopted for the transition in ^{16}O. The $B(E3)\uparrow$ found using $\beta_3 = 0.48$ is

TABLE I. Parameter values defining the $n + {}^{14}\mathrm{C}$ and $p + {}^{14}\mathrm{O}$ interaction. Potential strengths (V) are for coupling to both positive and negative parity states. λ are blocking strengths of occupied single-nucleon orbits, in MeV. Additionally, all states involve a λ strength of 10^6 for the $1s_{\frac{1}{2}}$ orbit. The numbers in brackets are the OPP values required to give the best representation of the three low excitation states in ^{15}F. Lengths are in fm.

V_0 (MeV)	−43.16
V_{ll} (MeV)	0.475
V_{ls} (MeV)	7.0
V_{ss} (MeV)	0.0

R_0 (fm)	a (fm)	R_c (fm)	a_c (fm)	w_c	β_2	β_3
3.083	0.63	2.59	0.6	−0.051	−0.36	−0.48

J^π	E ^{14}C	E ^{14}O	$\lambda_{p_{\frac{3}{2}}}$	$\lambda_{p_{\frac{1}{2}}}$
0_1^+	0.00	0.00	10^6	9.9 (9.42)
1_1^-	6.09	5.17	16.0	5.25
0_2^+	6.59	5.92	10^6	4.2
3_1^-	6.73	6.27	16.0	4.3 (11.75)
2_1^+	7.01	6.59	10^6	2.5 (2.9)

1323 $e^2\mathrm{fm}^6$ which compares with the adopted value of 1300 $e^2\mathrm{fm}^6$ for ^{16}O assessed from electron scattering data. For a full description of how the 3pF charge distribution is implemented in MCAS, see Refs. [18,41].

C. Parameter values for the nuclear interaction

A vibration collective model, as recently detailed [42], has been used to specify the matrices of interaction potentials with the clusters $^{15}\mathrm{C}$ ($n + {}^{14}\mathrm{C}$) and $^{15}\mathrm{F}$ ($p + {}^{14}\mathrm{O}$). The coupled-channel interaction matrices were formed using the five states in ^{14}C and ^{14}O as discussed above. They are listed again in Table I in which the strengths of the OPP terms required for each are given. The OPP scheme is one that allows for Pauli blocking or hindrance of the added nucleon to the core nucleus in forming the relevant compound nuclear system. The OPP strengths listed in Table I are those that lead to good results for the low excitation spectra for ^{15}C and ^{15}F. Those values, shown in brackets in the table, effect fine tuning of the energies of the ^{15}F levels, notably of the $\frac{1}{2}^-$ state. This may be a reflection of the differences between the spectra of the core nuclei ^{14}C and ^{14}O. This use of OPP strengths as parameters guided by occupancy levels will, in future works, be improved by stronger microscopic constraints. In Ref. [21], a microscopic cluster model has been studied as a guide for OPP strengths, with further work to be done to fully determine these strengths microscopically.

The calculations of the $^{15}\mathrm{F}$ ($p + {}^{14}\mathrm{O}$) system required addition of Coulomb interactions, and those were derived assuming that ^{14}O had the 3pF charge distribution given in Eq. (11).

III. ENERGY LEVELS OF THE MIRROR PAIR ^{15}C ($n + {}^{14}$C) AND ^{15}F ($p + {}^{14}$O)

The spectra of ^{15}C and of ^{15}F we have calculated are compared with the experimental values in Figs. 2 and 3 respectively. They are discussed in the following subsection. Then in Sec. III B the centroid energies and widths are listed in Tables II and III respectively.

A. Energy level diagrams

In Fig. 2, the known low-energy spectrum of ^{15}C (to ≈8 MeV excitation) is shown in the column identified by "Expt." The lowest eight states have known spin-parities. They are compared with the spectral results obtained with the vibration model describing the interactions of a neutron with the five states of the core nucleus, ^{14}C, shown in Fig. 1. All states other than the lowest two are resonances and can decay by neutron emission. The lowest six known states (to ≈5 MeV excitation in ^{15}C) are well matched by the theoretical results, save that the order of the close lying $\frac{5}{2}^-$ and $\frac{3}{2}^-$ resonances is interchanged. The energy of the ground state lies 1.217 MeV below the $n + {}^{14}\mathrm{C}$ threshold, in good agreement with the experimental value of 1.218 MeV.

As is evident in Fig. 3, little is known of the spectrum of ^{15}F, but the first three resonances have established spin-parity assignments consistent with the lowest three states in the mirror, ^{15}C. Five states of ^{14}O, the mirrors of those in ^{14}C, were used in the evaluations of ^{15}F. The known values of the excitation energies (four being resonance centroid energies), and the widths of those four resonances, were taken into account in the coupled-channel calculations. The relevant Hamiltonian was initially taken as that deemed best in giving

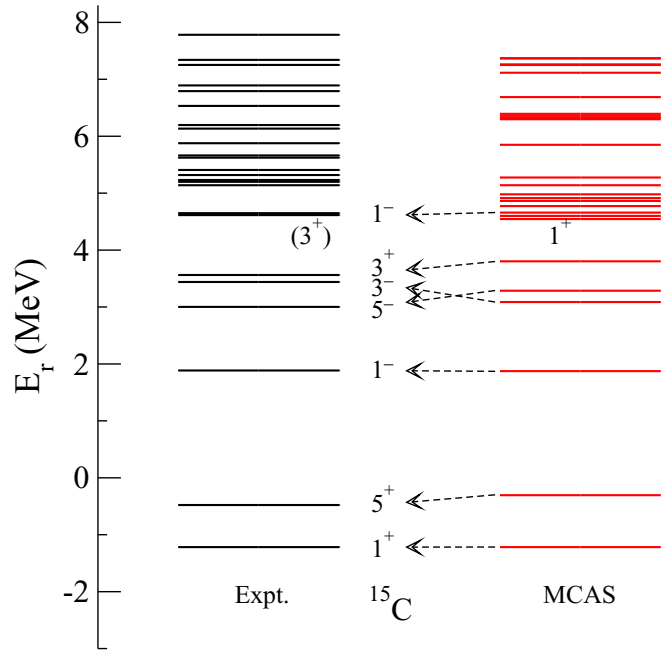

FIG. 2. Excitation spectra of ^{15}C in relation to the $n + {}^{14}$C threshold. The two nonresonant states are thus identified. The states are classified by twice their spin and their parity.

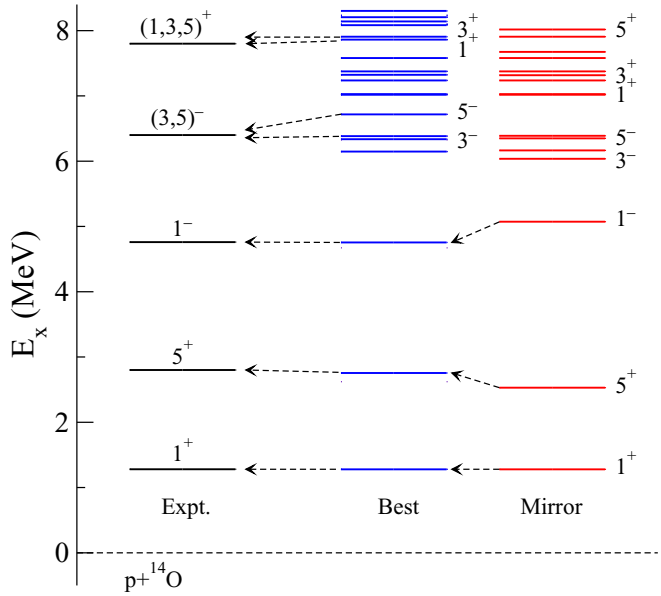

FIG. 3. Excitation spectra of ^{15}F in relation to the $p + {}^{14}$O threshold. The states are classified by twice their spin and their parity. The spectrum identified by "Mirror" was found using the defined $n + {}^{14}$C interaction modified only by inclusion of a Coulomb interaction associated with the 3pF charge distribution. The spectrum labeled "Best" also involved making the small changes to the OPP strengths, as explained in the text.

the spectrum of ^{15}C from the $n + {}^{14}$C cluster evaluation, with the addition of Coulomb interactions formed using the 3pF model of the charge distribution in ^{14}O. The results of that initial evaluation are those shown in Fig. 3 and labeled therein by "Mirror." There is reasonable comparison with the known spectrum ("Expt."). Small adjustments made by variation of the $\lambda_{p_{\frac{1}{2}}}$ values in the OPP set give the results identified as "Best." Importantly both evaluations lead to the ground state resonance lying at 1.279 MeV in the $p + {}^{14}$O center of mass. Clearly there are many more states predicted to lie in the spectrum above the three well established resonances.

As shown in Fig. 3, there appears to be a slight difference in the underlying nucleon shell occupancies of ^{15}C and ^{15}F, indicated in this model by slightly differing OPP values, $\lambda_{p_{\frac{1}{2}}}$, for three states in the mass-14 cores as listed in Table I.

B. Tabulated level energies and widths

The two lowest states in ^{15}C are subthreshold to neutron breakup but all other states are resonances. The widths determined by the MCAS evaluations are solely those for nucleon breakup of the mass-15 systems. With ^{15}F, the lowest two resonances only decay by proton emission, and the measured and calculated widths can be compared. We list the values for ^{15}C that are given in Ref. [31]. For the three lowest states in ^{15}F we have used the values assessed in a recent article [24], drawing a comparison with the ENSDF value for the ground state [43].

The coupled-channel (nuclear) interaction Hamiltonian and the OPP accounting for Pauli blocking and/or hindrance in the selected five states of ^{14}C were chosen to give an optimal match to the known lowest eight states in ^{15}C. To emphasise that, those with energies within ≈300 keV of the data are shown in boldface type in Table II. There are many more states predicted by this collective model evaluation. Above 5 MeV in the spectrum listed in Table II, the experimentally known resonances have ambiguous spin-parity assignments, though the richer evaluated spectra have characteristics consistent with those sets. The widths of the first two resonances are small and consistent with observation.

TABLE II. Spectra of ^{15}C. The experimental values, Expt., are compared with the MCAS results found using the vibration model. All resonance energy values, centroid E_r, and (full) width Γ values are in MeV. Theoretical energies within ≈300 keV of data are shown in boldface.

Expt.			MCAS		
J^π	E_r	Γ	J^π	E_r	Γ
$\frac{1}{2}^+$	**−1.218**		$\frac{1}{2}^+$	**−1.217**	
$\frac{5}{2}^+$	**−0.478**		$\frac{5}{2}^+$	**−0.3056**	
$\frac{1}{2}^-$	**1.885**	<0.040	$\frac{1}{2}^-$	**1.874**	0.019
$\frac{5}{2}^-$	**3.002**	<0.014	$\frac{5}{2}^-$	**3.287**	0.003
$\frac{3}{2}^-$	**3.439**		$\frac{3}{2}^-$	**3.088**	0.028
$\frac{3}{2}^+$	**3.562**	1.74	$\frac{3}{2}^+$	**3.802**	3.16
			$\frac{1}{2}^+$	4.545	0.218
			$\frac{3}{2}^-$	4.600	0.009
$(\frac{3}{2}^+)$	**4.615**	0.064	$\frac{3}{2}^+$	**4.980**	0.337
$\frac{1}{2}^-$	**4.648**		$\frac{1}{2}^-$	**4.648**	0.006
$(\frac{5}{2}, \frac{7}{2}, \frac{9}{2}^+)$	**5.14**	<0.02	$\frac{5}{2}^+$	**5.140**	0.297
			$\frac{5}{2}^-$	5.275	0.009
$(\frac{3}{2} \to \frac{7}{2})$	5.2	≈0.05	$\frac{1}{2}^+$	5.849	7×10^{-5}
			$\frac{7}{2}^-$	6.300	0.037
			$\frac{5}{2}^+$	6.232	0.032

The coupled-channel interaction potentials so found were then used to define a spectrum for ^{15}F. But, as described earlier, some essential changes to the input specifications had to be made. First, most states of the mirror core nucleus, ^{14}O, are resonances themselves and were used as such in the MCAS evaluations. The excitation energy centroids of those states differ slightly from the corresponding ones in ^{14}C. Then there are Coulomb interactions to be included with the p-^{14}O cluster evaluations. To find the best representation of the ^{15}F spectrum, small adjustments to the $\lambda_{p_{\frac{1}{2}}}$ OPP values were made, as indicated in Table I. The results are given in Table III, where they are compared with the limited known spectral values [13,24]. Comparing Tables II and III, we note that a difference in energy between the ground state and the $\frac{5}{2}^-$ state of 4.5 MeV in ^{15}C, and a difference of 5.4 MeV for ^{15}F. This is an example of the changes the addition of a Coulomb potential makes to the Hamiltonian; another such change is the resonance nature of the ^{15}F ground state.

TABLE III. Spectra of ^{15}F. The notation is as given in Table II, with theoretical energies within ≈300 keV of data shown in boldface. For the $\frac{1}{2}^+$ ground state, we provide the latest measured width and its statistical error, as well as the NNDC value. N.B.: In Ref. [13], Table I gives widths for their $(\frac{5}{2}, \frac{3}{2})^-$ state as 0.2(2); the text on page 10 indicates that 0.2 MeV is the experimental resolution.

Expt.				MCAS		
Ref.	J^π	E_r	Γ	J^π	E_r	Γ
[24]	$\frac{1}{2}^+$	**1.270**	0.376(0.070)	$\frac{1}{2}^+$	**1.282**	0.715
[43]	”	”	0.660			
[24]	$\frac{5}{2}^+$	**2.794**	0.30 ± 0.010	$\frac{5}{2}^+$	**2.757**	0.337
[24]	$\frac{1}{2}^-$	**4.757**	0.036 ± 0.014	$\frac{1}{2}^-$	**4.765**	0.107
				$\frac{3}{2}^-$	6.160	0.298
				$\frac{1}{2}^-$	6.347	0.523
				$\frac{3}{2}^-$	**6.391**	0.096
[13]	$(\frac{3}{2}, \frac{5}{2}^-)$	**6.4**	⩽0.2	$\frac{5}{2}^-$	**6.726**	0.074
				$\frac{1}{2}^+$	7.030	0.279
				$\frac{7}{2}^-$	7.069	0.273
				$\frac{5}{2}^-$	7.365	0.515
[13]	$(\frac{3}{2}, \frac{5}{2}^+)$	**7.8**	0.4 ± 0.4	$\frac{3}{2}^+$	**7.379**	0.487
				$\frac{1}{2}^-$	7.577	0.093
				$\frac{1}{2}^+$	7.836	3.229
				$\frac{3}{2}^+$	**8.076**	7.484
				$\frac{5}{2}^-$	8.217	0.552
				$\frac{7}{2}^-$	8.237	0.854
				$\frac{3}{2}^-$	8.782	0.893
				$\frac{5}{2}^+$	8.939	6.982
				$\frac{11}{2}^-$	9.422	0.785
				$\frac{3}{2}^-$	9.544	1.068
				$\frac{9}{2}^-$	9.589	0.902
				$\frac{7}{2}^-$	9.632	1.304
				$\frac{5}{2}^-$	9.652	1.137
				$\frac{5}{2}^+$	9.783	1.185
				$\frac{9}{2}^+$	10.344	1.078
				$\frac{3}{2}^+$	10.530	1.358
				$\frac{7}{2}^+$	10.534	1.223
				$\frac{1}{2}^-$	10.724	2.137
				$\frac{5}{2}^+$	10.758	1.679
				$\frac{1}{2}^+$	11.336	2.853

The three best determined resonances, centroid energies, and widths are quite well matched by the calculation results, as are the other two higher excitation resonances that have uncertain spin-parities and widths. The widths of the resonances calculated using MCAS are those solely for single-proton decay. However, the higher-lying resonances can also decay by two proton emissions so the widths given in Ref. [12] would include effects of that process.

IV. ^{14}O SCATTERING FROM HYDROGEN AT 180°

Using five states in the low excitation spectrum of ^{14}O, the ground (0_1^+), the 1^- (5.17 MeV), the 0_2^+ (5.92 MeV), the 3^- (6.27 MeV), and the 2^+ (6.59 MeV), our calculations gave the cross sections for p-^{14}O scattering at 180° that are compared with data [24] in Fig. 4. [Note that panel (c) of this figure relates to Sec. VI A.]

Semilogarithmic graphing emphasizes small structures in both data and evaluated results. This data clearly indicate three resonances; in [24] they are defined as the $\frac{1}{2}^+$ ground state of ^{15}F centered at 1.27 MeV with a width of 0.376/0.660 MeV, the $\frac{5}{2}^+$, first excited state, with a centroid and width of 2.794 and 0.301 MeV, and a $\frac{1}{2}^-$ resonance with centroid and width of 4.754 and 0.036 MeV respectively. The calculated results reproduce those three resonances very well. Panel (b) reveals that more structure is predicted for energies in the region above 6 MeV, where we anticipate that there exist groups of states of both parities. By studying correlations in two-proton emission from ^{16}Ne [13], two resonance aspects of ^{15}F were defined in that region, having centroids at 6.57 and 7.8 MeV excitation. However, their spin values and widths are uncertain as yet.

V. THE MIRROR PAIR ^{15}O ($n + ^{14}$O) AND ^{15}N ($p + ^{14}$C)

Being strongly bound, the spectra of the mirror pair ^{15}O and ^{15}N have been studied for many decades [44]. That of the better known ^{15}N was recently surveyed experimentally over a range of 15 MeV using the ^{14}N$(d, p)^{15}$N reaction [45], and in the same paper the COSMO shell model code [46] was used to successfully calculate these levels, up to 11.5 MeV. That investigation used an unrestricted $1p$–$2s1d$ shell valence space. Mirror states in the less-well-known ^{15}O spectrum were then suggested. Another shell model investigation using a lesser space, the $2s_{1/2}$ and $1d_{5/2}$ shells, soon followed [47].

Using MCAS, the nuclear interactions for the $n + ^{14}$O and $p + ^{14}$C systems are stronger than those required with the $p + ^{14}$O and $n + ^{14}$C calculations. That is evident from the much larger energies (13.223 and 10.207 MeV) of the relevant nucleon-core nucleus thresholds above the ground states of ^{15}O and ^{15}N respectively. That expectation also follows from the numbers of strong attractive (8) versus relatively weaker repulsive (6) two-nucleon interactions experienced by the extra-core nucleon in the clusters ^{15}N ($p + ^{14}$C) and ^{15}O ($n + ^{14}$O). In the clusters ^{15}C ($n + ^{14}$C) and ^{15}F ($p + ^{14}$O), in contrast, there are 6 strong attractive and 8 repulsive pairings. Additionally the OPP strengths for the ^{15}N and ^{15}O cases will differ from those of the ^{15}C and ^{15}F clusters since, with 6 rather than 8 extra core-like nucleons, the single-nucleon shell occupancies of those nucleons in the core nuclei are expected to be lesser.

We have used the MCAS approach to optimally find the subthreshold levels in ^{15}O treated as the $n + ^{14}$O cluster and especially to find that the ground state lies 13.22 MeV below the neutron emission threshold. This threshold lies well above those for emission of a proton (7.30 MeV), an α (10.22 MeV), and a ^{3}He (12.08 MeV). Thus, while our calculations lead to

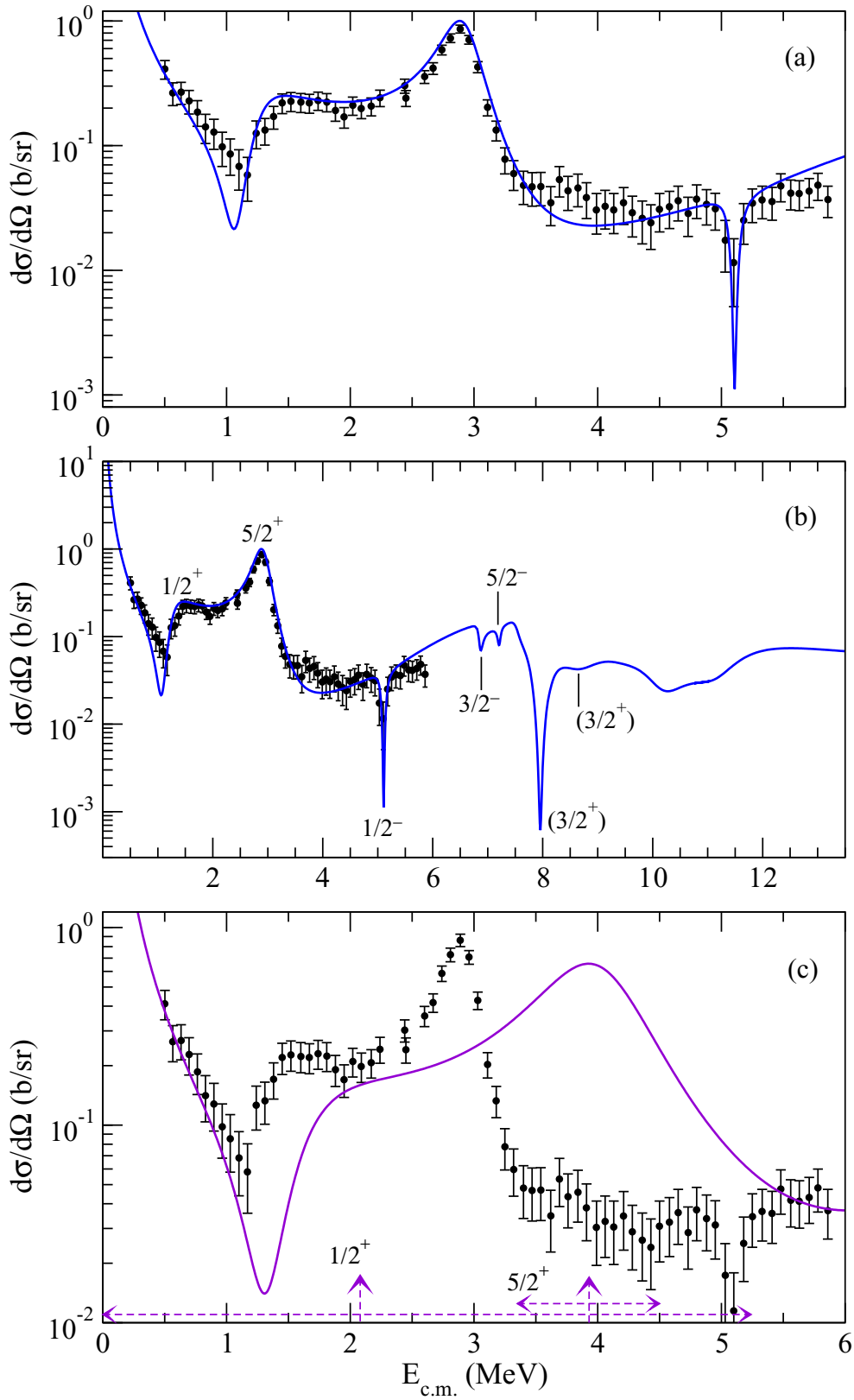

FIG. 4. (a) The 180° cross section data of [24] compared with MCAS results. The measured data are compared with cross sections evaluated using the vibrational model to specify the matrix of interaction potentials for a proton-^{14}O cluster. Five states of the core as described in text were used. (b) The same calculation over a larger energy range, predicting resonance features at energies above those measured. (c) Another calculation of the cross section found with solely the proton-ground state potential, to illustrate channel-coupling effects. Dashed lines indicate theoretical energy centroids and widths determined by resonance location routine (see Ref. [30]).

TABLE IV. Parameter values defining the $n + {}^{14}$O and $p + {}^{14}$C interaction interactions. Potential strengths (V) are for coupling to both positive and negative parity states. λ are blocking strengths of occupied single-nucleon orbits, in MeV.

V_0 (MeV)			−57.0	
V_{ll} (MeV)			0.475	
V_{ls} (MeV)			7.0	
V_{ss} (MeV)			0.0	
R_0 (fm)	a (fm)	β_2	β_3	
3.083	0.63	−0.36	−0.48	
J^π	E ^{14}O	E ^{14}C	$\lambda_{1s_{\frac{1}{2}}}$	$\lambda_{1p_{\frac{3}{2}}}$	$\lambda_{1p_{\frac{1}{2}}}$
0^+_1	(0.00)	(0.00)	10^6	17.5	2.8
1^-_1	(5.17)	(6.09)	10^6	17.5	1.25
0^+_2	(5.92)	(6.59)	10^6	17.5	3.5
3^-_1	(6.27)	(6.78)	10^6	17.5	1.6
2^+_1	(6.59)	(7.01)	10^6	17.5	1.7

12 subthreshold (to neutron emission) levels, only the most bound set of 6 are not resonances for emission of the other nuclear particles. Empirically there are 7 actual subthreshold bound states in ^{15}O while there are ≈40 resonant states above those and below the neutron emission threshold. On the other hand, the proton emission threshold in the mirror system, ^{15}N, is the first of such and lies 10.207 MeV above the ground. Empirically, there are 17 subthreshold (bound) states in ^{15}N.

A. Specifics of the ^{15}O and ^{15}N evaluations

The nuclear interaction and the OPP weights to account for Pauli blocking of single-nucleon states was specified by finding as good a spectrum for ^{15}O ($n + {}^{14}$O) as possible. In particular, we sought the ground state of correct spin-parity and energy below the neutron emission threshold and the first two excited states in the correct order and with good energy values. The coupled-channel Hamiltonian was formed using the five states of the target nucleus ^{14}O as used before (and of ^{14}C in the case of ^{15}N). The geometry, V_{ls}, and V_{ll} values were set at those determined from our study of the other mass-15 isobars, ^{15}C and ^{14}F. However, for the reasons discussed above, the central interaction strength was varied, with −57.0 MeV being found appropriate. The parameter values of the OPP used for the two systems are listed in Table IV.

For the ^{15}N calculation, Coulomb interactions were added to the nuclear ones and the appropriate set of state energies in ^{14}C were used. In this case, the Coulomb interactions were constrained by using a charge distribution that matches the known root-mean-square (rms) charge radius. For ^{14}C that value is $R^{(c)}_{\rm rms} = 2.56 \pm 0.05$ fm [40], defined using a modified Harmonic oscillator (MHO) model for the charge distribution of ^{14}C to analyze an electron scattering form factor in the momentum range 1.04 to 2.16 fm^{-1}.

We have used the three parameter Fermi (3pF) model for the charge distribution. Sets of parameter values ranging between those reported [40] from analyses of electron scattering data from ^{12}C and from ^{16}O were determined by the distributions having the charge rms radius of 2.56 fm for ^{14}C. That set of parameters are listed in Table V. The first three parameter sets, (a), (b), and (c), in Table V are one-parameter variations on the 3pF model parameters for the adopted charge distribution in ^{12}C [40] that give $R^{(c)}_{\rm rms} = 2.56$ fm. The sets (d), (e), and (f) kept $R_c = 2.355$ fm, varied a_c, and adjusted w_c to find the same $R^{(c)}_{\rm rms}$. The last set in Table V kept $a_c = 0.5$ fm, varied R_c, and adjusted w_c to have the same result. Thus there are quite diverse sets of parameters for this model giving the known rms charge radius. As shown in Refs. [18,41], it is the value of $R^{(c)}_{\rm rms}$ that affects the Coulomb contribution, with the specific values of R_c, a_c, and w_c leading to that $R^{(c)}_{\rm rms}$ having only minor impact on results. Coupled-channel evaluations using each of these 3pF sets were made and the spectra found were all very similar. The last column in Table V lists the value of the ground state energies so found, showing a difference of at most 20 keV.

TABLE V. Parameter values for a 3pF model of the charge distribution in ^{14}C that give $R^{(c)}_{\rm rms} = 2.56$ fm and the ground state energies from MCAS calculations of the $p + {}^{14}$C system.

ID	R_c (fm)	a_c (fm)	w_c	$E_{\rm g.s.}$(^{15}N)
(a)	2.355	0.5224	−0.08	−10.200
(b)	2.355	0.6	−0.149	−10.209
(c)	2.52	0.5224	−0.149	−10.206
(d)	2.355	0.5	−0.04	−10.199
(e)	2.355	0.54	−0.1	−10.203
(f)	2.355	0.64	−0.15	−10.232
(g)	2.425	0.5	−0.06	−10.208
(h)	2.525	0.5	−0.09	−10.222
(i)	2.536	0.5	−0.1	−10.220

B. The spectra of ^{15}O and ^{15}N

The low-excitation spectra of the mirror pair ^{15}O and ^{15}N are depicted in Fig. 5. Those for ^{15}O are shown on the left and those for ^{15}N on the right. The excitation energies are shown relative to the nucleon separation thresholds (13.223 MeV for $n + {}^{14}$O and 10.207 MeV for $p + {}^{14}$C). The calculated spectrum for ^{15}N displayed was found using the 3pF model parameter set (h) in Table V. The known states, given in the columns labeled "Expt.", were taken from [31]. The calculated spectra are identified by the label "MCAS."

The calculated results for ^{15}O closely match most known states to 10 MeV excitation, though there are many more levels that lie ≈10 MeV and greater above the ground. Notably, the ground state is found to within a keV of its known energy below the neutron emission threshold, the doublet of states at ≈ − 8 MeV binding are found in the correct order, and the next five known states in the spectrum have calculated partners with energies within a few hundred keV of the known values. The $\frac{3}{2}^+$ plays an important role in the ^{14}N(p,γ) radiative capture reaction as part of the the CNO cycle. This is overbound in the calculation by 750 keV.

With that nuclear interaction, using the appropriate energies of the same five target states (in ^{14}C), and the 3pF

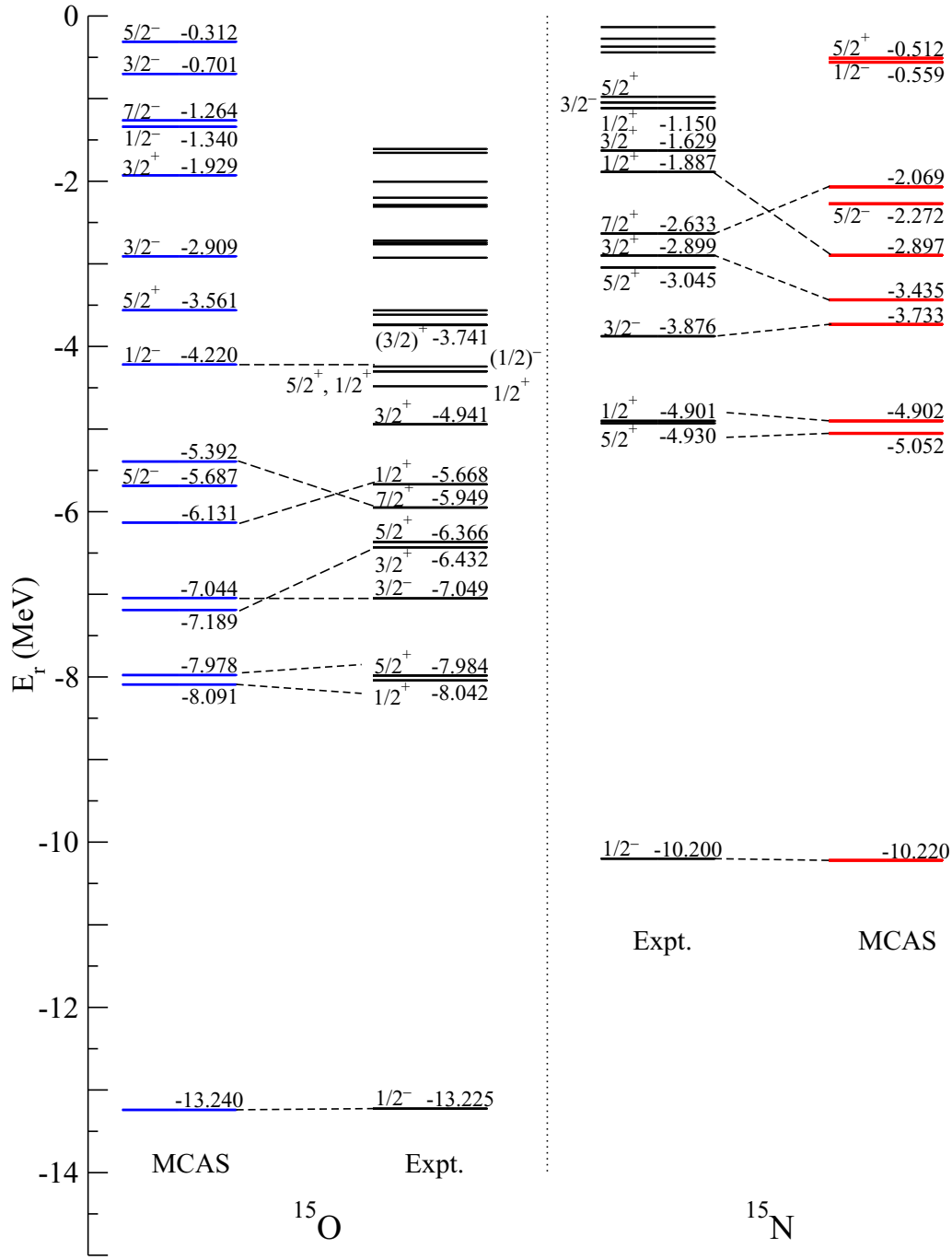

FIG. 5. The subthreshold spectra of ^{15}O (left) and of ^{15}N (right) found using MCAS compared to the experimental values.

charge distribution with the parameters of set (h) in Table V, the single calculation leads to the spectrum for ^{15}N that is compared with the known one in the right side of Fig. 5. The ground state was found to be -10.22 MeV below the proton emission threshold, in good agreement with the known value, and the low lying spectrum again reasonably matched. The $\frac{5}{2}^+|_1$ state now is more bound than the $\frac{1}{2}^+|_1$ one, as is the case in the experimental spectrum, and the splitting of that doublet is larger than observed. The next two states in the known spectrum of ^{15}N have matching partners from the calculation, both lying within a few hundred keV of the appropriate energies. Also the known $\frac{7}{2}^+$ state has a calculated partner in close agreement, but the $\frac{5}{2}^+|_2$ state is calculated to be at ≈ -0.5 MeV, not at ≈ -3 MeV as in the experimental spectrum.

The known spectra of both mass-15 isobars are much richer than those we have evaluated, but only for reasonably large excitations, reflecting the simplicity of the model chosen to define the coupled-channel Hamiltonian, with the number of core nuclear states considered and use of the purest of vibration models for the structure and interactions.

VI. CHANNEL-COUPLING EFFECTS IN THE POTENTIALS USED

In this section, we examine the magnitude of channel coupling in the closely related potentials used to investigate the $n + {}^{14}\mathrm{O}$ / $p + {}^{14}\mathrm{C}$ and $p + {}^{14}\mathrm{O}$ / $p + {}^{14}\mathrm{C}$ mirror systems. We consider the effect of the channels included, and that of the Pauli-hindrance strengths.

Considering the p-^{14}O system, the coupled-channel calculation which produced a good match to the properties of the three well established ^{15}F resonance states yielded many more resonances. As listed in Table III, to 10 MeV excitation the calculation gave 24 resonances, of which

3 are $\frac{1}{2}^+$ resonances, the ground (1.28 MeV) and 7.030 MeV being the first two;
3 are $\frac{1}{2}^-$ resonances, the 4.765 and 6.347 MeV being the first two;
3 are $\frac{3}{2}^+$ resonances, the 7.379 and 8.076 MeV being the first two;
4 are $\frac{3}{2}^-$ resonances, the 6.160 and 6.391 MeV being the first two;
3 are $\frac{5}{2}^+$ resonances, one at 2.757 and the second near 9 MeV excitation;
4 are $\frac{5}{2}^-$ resonances; the 6.726 and 7.365 MeV being the first two;
3 are $\frac{7}{2}^-$ resonances, the 7.069 and 8.237 MeV being the first two;

and an $\frac{11}{2}^-$ resonance at 9.422 MeV excitation.

These result from the calculation in which five states of the core nucleus (quantum label I) were used. Pauli blocking of the extra-core proton into the $1s_{\frac{1}{2}}$ orbit was assumed for all five states, as was the $1p_{\frac{3}{2}}$ orbit in the 0_1^+, 0_2^+, and 2^+ states (as shown in Table I). That orbit was only Pauli hindered in the 1^- and 3^- states. In all five states, however, the $1p_{\frac{1}{2}}$ orbit was only Pauli hindered. Consequently, in the coupled-channel calculation the important channels, uniquely defined for each total spin-parity J^π of the cluster by the quantum number set $[(nl)j \otimes I]; J^\pi$, are those involving attachment of a proton in the $1p_{\frac{1}{2}}$ orbit and, selectively, in the $1p_{\frac{3}{2}}$ orbit.

A. The effects of included channels

Considering first the individual aspects of the the p-^{14}O system coupled-channel calculations, the nuclear interactions for each incident channel support three single-proton bound states, for the $1s_{\frac{1}{2}}$; $1p_{\frac{3}{2}}$, and $1p_{\frac{1}{2}}$ orbits. With the ground state interaction, those single-proton state energies are -17.71, -5.97, and -2.51 MeV respectively. Similar values are found in the interaction with each excited state of ^{14}O. Coupling a proton in the allowed p orbits (the OPP forbids coupling to the $1s_{\frac{1}{2}}$ orbit) leads to the set of channels for the coupled-channel evaluations of the J^π values of the known three resonances that are listed in Table VI.

The interactions also support single-proton resonance states which form additional components within the description of relevant J^π resonance wave functions of ^{15}F. Notably, in the single-proton spectrum from the proton-^{14}O ground-state interaction there is a $2s_{\frac{1}{2}}$ resonance with E_r, $(\Gamma) = 2.076$, (4.326) MeV and a $1d_{\frac{5}{2}}$ one at 3.963, (1.155) MeV. These both form allowable components on coupling with the states of ^{14}O. Being resonances themselves, these two single-particle attributes are not Pauli influenced. An example of an additional channel in the $J^\pi = \frac{1}{2}^+$ Hamiltonian matrix is that for the coupling $1d_{\frac{5}{2}} \otimes 2_1^+$. However, with the possible exception of the couplings of these $2s_{\frac{1}{2}}$ and $1d_{\frac{5}{2}}$ resonances to the ground state of ^{14}O in the description of the two positive-parity resonances in ^{15}F, other cluster components so formed are not expected to be dominant in the description of the three known ^{15}F resonance states. This expectation results because the centroid values of the single-proton resonances are many MeV above those of the proton (p-shell) bound states. Primarily they would influence what results at higher excitation energies and, for example, only the $1d_{\frac{5}{2}} \otimes 3^-$ coupling produces the $\frac{11}{2}^-$ state that we find at 9.422 MeV excitation.

TABLE VI. Channels formed with the p-shell bound states and core nucleus states used in calculating the three states of ^{15}F.

J^π	$1p_{\frac{3}{2}}$	$1p_{\frac{3}{2}}$	$1p_{\frac{1}{2}}$	$1p_{\frac{1}{2}}$
	$\otimes$	$\otimes$	$\otimes$	$\otimes$
$\frac{1}{2}^+$	1^-		1^-	
$\frac{5}{2}^+$	3^-	1^-	3^-	
$\frac{1}{2}^-$	2^+		0_1^+	0_2^+

As the n-^{14}O system used a potential very similar to that of the p-^{14}O, calculations have been made to dissect the effects of channel coupling in its MCAS evaluations. The diverse resulting low excitation spectra for ^{15}O are displayed in Fig. 6.

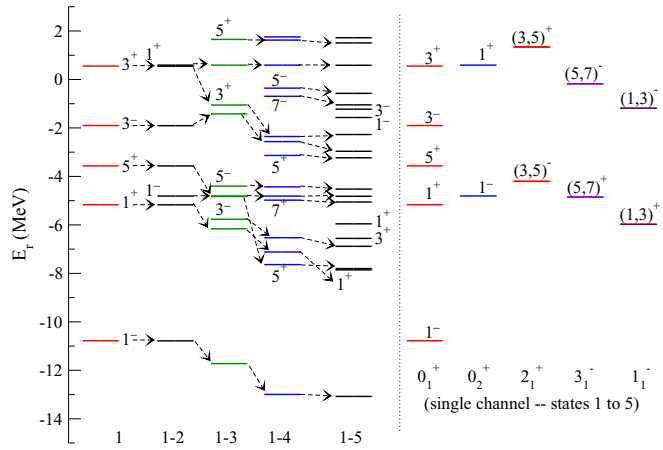

FIG. 6. Changes wrought by adding channels in the calculation (left-hand side) and low lying states formed when only the individual target states are used in calculations (right-hand side). The individual states of each spectrum have been labeled with twice their spin and parity values.

TABLE VII. The effects of the OPP values on the centroids and widths found for the three resonances in ^{15}F.

			Half		Full	
OPP	^{14}O I^π	^{15}F J^π	E_r	Γ	E_r	Γ
$1p_{\frac{1}{2}}$	$\otimes 0^+_1$	$\frac{1}{2}^-$	0.858	0.010	4.755	0.106
	$\otimes 0^+_2$	$\frac{1}{2}^-$	4.728	0.108	4.755	0.106
	$\otimes 3^-$	$\frac{5}{2}^+$	2.600	0.271	2.651	0.336
	$\otimes 1^-$	$\frac{1}{2}^+$	1.244	0.634	1.280	0.708
$1p_{\frac{3}{2}}$	$\otimes 3^-$	$\frac{5}{2}^+$	2.588	0.267	2.651	0.336
	$\otimes 1^-$	$\frac{1}{2}^+$	1.236	0.631	1.280	0.708
	$\otimes 1^-$	$\frac{5}{2}^+$	2.712	0.316	2.651	0.336

Shown therein, on the left-hand side, are the results obtained using select sets of the target states according to the sequence

1: Just the ground state of ^{14}O was used.
1-2: The two 0^+ states were included.
1-3: The three positive parity states $(0^+_1, 0^+_2, 2^+_1)$ were used.
1-4: The three positive parity states plus the 3^- state of ^{14}O were taken into account.
1-5: The full (five state) result.

On the right-hand side, the spectra found using each target state by itself are shown with the spin-parity (J^π_n) identifying each of the five chosen target states. These states are the basis in specifying the full coupled-channel matrices.

As each target state is included in the coupled-channel calculation (the left-hand panel of results) the resulting spectra becomes more complex with new spin-parity entries and many, especially the ground state, being progressively more bound. Clearly channel coupling is essential in finding a spectrum for ^{15}O that resembles the known low-excitation states.

To further emphasise the importance of coupled-channel effects in these evaluations, and to identify significant components relating to the values obtained for the low energy spectrum of ^{15}F and p-^{14}O cross sections, we have made single-channel calculations using solely the ground state interaction. The single-state (ground state potential) calculation gave the cross section that is compared with the data [24] in panel (c) of Fig. 4. The agreement with the data is poor but the basic information on the spin-parities of the three defined resonances in the energy range is correctly reproduced. This suggests the the ground state couplings with the $2s_{\frac{1}{2}}$ and $1d_{\frac{5}{2}}$ proton resonance states do influence results of the full coupled-channel calculation. That the $2s_{\frac{1}{2}}$ single-proton resonance lies below the $1d_{\frac{5}{2}}$ one is due to the v_{ll} term in the interactions.

B. OPP effects

Finally, a series of coupled-channels calculations were made changing the values of the p-shell OPP in the p-^{14}O individually. The effects on the calculated energies of the three resonance states of interest in ^{15}F, the ground and first two known excited states, are shown in Table VII. Each calculation halved an individual value of the OPP and the resulting energies, both centroids and widths, are compared with the unchanged coupled-channel values in the columns designated "Half" and "Full". These OPP changes, as well as those with the 2^+ target state, also affect the results for other resonances in the evaluated spectrum. For the three known resonances, clearly the most significant element is the OPP value for the $1p_{\frac{1}{2}}$ orbit in the ground state of ^{14}O. Halving that OPP strength (to 4.71 MeV) has caused the $\frac{1}{2}^-$ state in ^{15}F to become the ground and have a tenth of the "Full" calculation width. The other changes cause less than 100 keV change to the energy centroids and widths.

VII. CONCLUSIONS

Mirror symmetry for nuclear interactions has been used to study the spectra of the mass-15 isobars ^{15}C, ^{15}N, ^{15}O, and ^{15}F. The MCAS method has been used to evaluate their low-energy (to ≈10 MeV) excitation spectra considering each to be a cluster of a nucleon with either of the mirrors ^{14}C and ^{14}O. There are two mirror pairs in these mass-15 isobars, ^{15}O and ^{15}N, and ^{15}C and ^{15}F, which are distinct in that the former are well bound with many uniquely bound states in their spectra, while of the latter pair ^{15}C is weakly bound with just two subthreshold states and its mirror, ^{15}F, lies beyond the proton drip-line.

In the evaluations, the lowest five states in the core nuclei ^{14}C and ^{14}O were used to form coupled-channel interactions based upon a collective (vibration) model description of the core nuclei. First we sought the spectra of ^{15}C (as the $n + {}^{14}$C cluster). With the set of parameter values for the Hamiltonian that gave a best match to the known spectrum of ^{15}C (to ≈6.5 MeV excitation), the addition of Coulomb terms led to a reasonable match of the spectrum of ^{15}F (as the $p + {}^{14}$O cluster). The Coulomb interactions were generated using a three-parameter Fermi model for the charge distribution in ^{14}O. The same basic nuclear potential, modified only in central well depth and with OPP strengths reflecting the changes in like-nucleon shell occupancies in the cores, was used to evaluate the spectra of the other mass-15 isobar pair ^{15}O and ^{15}N. With this essentially single potential matrix in the Hamiltonians, very good agreement was obtained for the low-energy spectra of ^{15}O and ^{15}N.

Finally, as the MCAS procedure produces scattering phase shifts for ^{14}O$(p, p)^{14}$O scattering, and in light of recent data, the elastic scattering cross section calculation reported in a previous Letter [8] has been updated. Very good agreement has been found between all three known resonance features and the nonresonant scattering background. These calculated results suggest that scattering cross sections when measured at higher energies (7–9 MeV for example) should reveal more structure (resonance states) in the exotic nucleus ^{15}F.

ACKNOWLEDGMENT

S.K. acknowledges support from the National Research Foundation of South Africa.

[1] L. V. Grigorenko, I. G. Mukha, I. J. Thompson, and M. V. Zhukov, Phys. Rev. Lett. **88**, 042502 (2002).
[2] K. W. Brown *et al.*, Phys. Rev. Lett. **113**, 232501 (2014).
[3] L. V. Grigorenko, T. A. Golubkova, and M. V. Zhukov, Phys. Rev. C **91**, 024325 (2015).
[4] V. Z. Goldberg, G. G. Chubarian, G. Tabacaru, L. Trache, R. E. Tribble, A. Aprahamian, G. V. Rogachev, B. B. Skorodumov, and X. D. Tang, Phys. Rev. C **69**, 031302(R) (2004).
[5] D. Baye, P. Descouvemont, and F. Leo, Phys. Rev. C **72**, 024309 (2005).
[6] F. Q. Guo *et al.*, Phys. Rev. C **72**, 034312 (2005).
[7] H. T. Fortune and R. Sherr, Phys. Rev. C **72**, 024319 (2005).
[8] L. Canton, G. Pisent, J. P. Svenne, K. Amos, and S. Karataglidis, Phys. Rev. Lett. **96**, 072502 (2006).
[9] H. T. Fortune and R. Sherr, Phys. Rev. Lett. **99**, 089201 (2007).
[10] L. Canton, G. Pisent, J. P. Svenne, K. Amos, and S. Karataglidis, Phys. Rev. Lett. **99**, 089202 (2007).
[11] I. Mukha *et al.*, Phys. Rev. C **77**, 061303(R) (2008).
[12] I. Mukha, N. K. Timofeyuk, K. Summerer, L. Acosta, M. A. G. Alvarez, E. Casarejos, A. Chatillon, D. Cortina-Gil, J. M. Espino, A. Fomichev, J. E. Garcia-Ramos, H. Geissel, J. Gomez-Camacho, L. Grigorenko, J. Hofmann, O. Kiselev, A. Korsheninnikov, N. Kurz, Y. Litvinov, I. Martel, C. Nociforo, W. Ott, M. Pfutzner, C. Rodriguez-Tajes, E. Roeckl, M. Stanoiu, H. Weick, and P. J. Woods, Phys. Rev. C **79**, 061301(R) (2009).
[13] I. Mukha *et al.*, Phys. Rev. C. **82**, 054315 (2010).
[14] H. T. Fortune, Phys. Rev. C **83**, 024311 (2011).
[15] M. G. Pellegriti *et al.*, Phys. Lett. B **659**, 864 (2008).
[16] F. Wamers *et al.*, Phys. Rev. Lett. **112**, 132502 (2014).
[17] A. Gade *et al.*, Phys. Lett. B **666**, 218 (2008).
[18] P. R. Fraser *et al.*, J. Phys. G **43**, 095104 (2016).
[19] N. K. Timofeyuk, B. Fernandez-Dominguez, P. Descouvemont, W. N. Catford, F. Delaunay, and J. S. Thomas, Phys. Rev. C **86**, 034305 (2012).
[20] B. Fernandez-Dominguez, X. Pereira-Lopez, N. K. Timofeyuk, P. Descouvemont, W. N. Catford, and F. Delaunay, Phys. Rev. C **91**, 024307 (2015).
[21] Y. A. Lashko, G. F. Filippov, and L. Canton, Ukr. J. Phys. **60**, 406 (2015).
[22] F. de Oliveira Santos *et al.*, in *The 4th International Conference on Proton Emitting Nuclei and Related Topics, June 2011, Bordeaux*, edited by B. Blank, AIP Conf. Proc. No. 1409 (AIP, New York, 2011), p. 134.
[23] F. de Oliveira Santos *et al.*, EPJ Web Conf. **17**, 06003 (2011).
[24] F. de Grancey *et al.*, Phys. Lett. B **758**, 26 (2016).
[25] A. Mercenne, Ph.D. thesis, Université de Caen Normandie, 2016 (unpublished).
[26] Y. Jaganathen, N. Michel, and M. Płoszajczak, Phys. Rev. C **89**, 034624 (2014).
[27] L. Canton, G. Pisent, J. P. Svenne, D. van der Knijff, K. Amos, and S. Karataglidis, Phys. Rev. Lett. **94**, 122503 (2005).
[28] K. Amos, L. Canton, P. R. Fraser, S. Karataglidis, J. P. Svenne, and D. van der Knijff, Nucl. Phys. A **912**, 7 (2013).
[29] K. Amos, S. Karataglidis, D. van der Knijff, L. Canton, G. Pisent, and J. P. Svenne, Phys. Rev. C **72**, 064604 (2005).
[30] K. Amos, L. Canton, G. Pisent, J. P. Svenne, and D. van der Knijff, Nucl. Phys. A **728**, 65 (2003).
[31] F. Ajzenberg-Selove, Nucl. Phys. A **523**, 1 (1991).
[32] P. Fraser, K. Amos, L. Canton, G. Pisent, S. Karataglidis, J. P. Svenne, and D. van der Knijff, Phys. Rev. Lett. **101**, 242501 (2008).
[33] L. Canton, P. R. Fraser, J. P. Svenne, K. Amos, S. Karataglidis, and D. van der Knijff, Phys. Rev. C **83**, 047603 (2011).
[34] P. R. Fraser *et al.*, Phys. Rev. C **94**, 034603 (2016).
[35] Y. H. Lam, N. A. Smirnova, and E. Caurier, Phys. Rev. C **87**, 054304 (2013), and references cited therein.
[36] N. B. Gove and M. Martin, At. Data Nucl. Data Tables **10**, 205 (1971).
[37] S. Karataglidis, Ph.D. thesis, The University of Melbourne, 1995 (unpublished).
[38] S. Raman, C. W. Nestor, and P. Tikkanen, At. Data Nucl. Data Tables **78**, 1 (2001).
[39] R. H. Spear, At. Data Nucl. Data Tables **42**, 55 (1989).
[40] H. de Vries, C. W. de Jager, and C. de Vries, At. Data Nucl. Data Tables **36**, 495 (1987).
[41] P. R. Fraser *et al.*, Eur. Phys. J. A **51**, 110 (2015).
[42] J. P. Svenne, L. Canton, K. Amos, P. R. Fraser, S. Karataglidis, G. Pisent, and D. van der Knijff, Phys. Rev. C **95**, 034305 (2017).
[43] J. Kelley, T. Truong, and C. G. Sheu, ENSDF (17/07/16).
[44] L. D. Wyly, Phys. Rev. **76**, 316 (1949).
[45] C. E. Mertin, D. D. Caussyn, A. M. Crisp, N. Keeley, K. W. Kemper, O. Momotyuk, B. T. Roeder, and A. Volya, Phys. Rev. C **91**, 044317 (2015).
[46] A. Volya, Phys. Rev. C **79**, 044308 (2009).
[47] H. T. Fortune, Phys. Rev. C **94**, 024339 (2016).